Available online at www.sciencedirect.com
SCIENCE DIRECT®
Journal of the European Ceramic Society 25 (2005) 1133–1142
www.elsevier.com/locate/jeurceramsoc

Crystallization and properties of glasses based on diopside–Ca-Tschermak's–fluorapatite system

Samia N. Salama, H. Darwish*, H. A. Abo-Mosallam

Glass Research Department, National Research Centre, El-Behoos St., Dokki, Cairo, Egypt

Received 8 January 2004; received in revised form 31 March 2004; accepted 16 April 2004
Available online 10 July 2004

Abstract

The crystallization characteristics of glasses based on compositions in the diopside [$CaMgSi_2O_6$]–Ca-Tschermak's [$CaAl_2SiO_6$]–fluorapatite [$Ca_5(PO_4)_3F$] system have been investigated. The effect of Ca-Tschermak's/diopside replacement, at constant $Ca_5(PO_4)_3F$ content, on the crystallization characteristics of the glasses and the solid solution phases formed, as well as the resulting microstructure, are traced by differential thermal analysis (DTA), X-ray diffraction analysis (XRD) and scanning electron microscopy (SEM).

Various pyroxene solid solutions together with fluorapatite phases are detected by XRD analysis. There is a preferential tendency for diopside to capture Ca-Tschermak's in its structure forming pyroxene solid solution of diopsidic type. The maximum concentration of $CaAl_2SiO_6$ that could be accommodated in the diopside structure was 25%. Above this percentage, gehlenite $Ca_2Al_2SiO_7$ also developed. However, there was no solid solution formed between pyroxene and fluorapatite.

The thermal expansion coefficients (α-values) and microhardness of the glasses and glass–ceramics were determined. The data of the glasses were correlated to the internal structure of the glasses, nature and role played by glass forming cations. However, the properties of the crystalline glasses were mainly attributed to different factors including the crystalline phases formed, residual glassy phase and the microstructures.

Keywords: Ca-Tschermak; Glass; Ceramic; Diopside; Microstructure

1. Introduction

It is well known that[1] compositions crystallizing to give solid solution series are important to control the properties of the resultant materials and offer an excellent opportunity to the glass–ceramic study. The casting properties of the glass–ceramics are improved by the presence of high content of pyroxene phases. Minerals capable of wide isomorphous substitution in their crystal structure and having the necessary physical and chemical characteristics, such as pyroxenes, may form the basis for production of many crystalline and glass–ceramic materials.[2]

Erol et al.,[3] succeeded to prepare glass–ceramic based on CaO–MgO–SiO_2–Al_2O_3 system. In this holocrystalline materials the only crystallized phase was diopside solid solution [$Ca(Mg,Al)(Si,Al)_2O_6$]. The result indicated that the produced glass ceramic has a fine and homogenous-grained microstructure.

The system $Ca_5(PO_4)_3F$–$CaMgSi_2O_6$ provides fundamental knowledge for the development of new kinds of ceramics, glasses and bioglass-ceramics. Furthermore, the high temperature relationship between apatite and diopside are very important from the geoscience point of view, since the components of the binary system are widespread rock-forming minerals.[4] It is claimed that the $Ca_5(PO_4)_3F$–$CaMgSi_2O_6$ glass–ceramics show a combination of high mechanical strength, a good chemical resistance and a good biocompatibility. A variety of glass–ceramics containing fluorapatite have been developed during the last years for biomedical and dental applications.[5–7] Apatite structures $Ca_{10}(PO_4)_6F_x(OH)_{2-x}$, where ($x$) is the fraction of OH-replacement by F^-, are the basic composition for a variety of important bioactive ceramics.[8]

The aim of the present work was to focus on the crystallization characteristics, solid solutions formed and

* Corresponding author. Fax: +20 2 3370931.
E-mail address: hussein25@yahoo.com (H. Darwish).

0955-2219/$ – see front matter.
doi:10.1016/j.jeurceramsoc.2004.04.025

microstructure of glass–ceramics based on diopside–Ca-Tschermak's–fluorapatite system with minor additions of Na_2O, B_2O_3 and TiO_2 with the object to provide fundamental knowledge for the type of multi-phase solid solutions of the studied glass–ceramic materials and studying their thermal expansion and microhardness properties.

2. Experimental techniques

2.1. Batch composition and preparation

The glass compositions were calculated to give different proportions of diopside [$CaMgSi_2O_6$]–Ca-Tschermak's [$CaAl_2SiO_6$]–fluorapatite [$Ca_5(PO_4)_3F$]. The calculated weight percentages of Ca-Tschermak's were gradually increased from 0 to 25% at the expense of diopside and at constant content of fluorapatite. Details of the glass oxide constituents are given in Table 1. Minor amounts of B_2O_3, Na_2O and TiO_2 were also added to the batch as 0.5, 2.0 and 1.0 g, respectively, for 100 g glass oxide constituents in the batch composition to facilitate the melting process and increase the crystallization tendency of the glasses.

Reagent grade powders of $CaCO_3$, SiO_2 (quartz), $MgCO_3$, $Al(OH)_3$, $NH_4H_2PO_4$, CaF_2, Na_2CO_3, H_3BO_3 and TiO_2 forming the glass batches were melted in a covered Al_2O_3-crucible in an electric furnace with SiC heating elements at 1450–1550 °C for 4 h. Melting was continued until a clear homogeneous melt was obtained; this was achieved by swirling the melt several times at about 30 min intervals. The melt was cast into rods and as buttons, which were then properly annealed in a muffle furnace at 650 °C for 1 h then cooled at 1 °C/min to room temperature to minimize the strain.

2.2. Differential thermal analysis

The thermal behaviour of the finely powdered (45–75 μm) glass samples was examined using a (NETZCH Geratebau GmbH Sleb Bestell-Nr. 348, 472 °C). The powdered sample was heated in Pt-holder against another Pt-holder containing α-Al_2O_3 as a standard material. A uniform heating rate of 10 °C/min was adopted up to the appropriate temperature of the glasses. The results obtained were used as a guide for determining the heat-treatment temperatures applied to induce crystallization.

2.3. Thermal treatment

The progress of crystallization in the glasses was followed using double stage heat-treatment regimes. Crystallization was carried out at temperatures in the region of the main DTA exothermic peak determined for each glass. The glasses were first heated according to the DTA results at the endothermic peak temperature for 5 h, which was followed by another thermal treatment at the exothermic peak temperature for 10 h.

2.4. Material investigation

Identification of crystal phases precipitating due to the course of crystallization was conducted by the X-ray diffraction patterns using a Philips type diffractometer (P.W. 1730) with Ni-filtered Cu Kα radiation. The crystallization characteristics and internal microstructures of the resultant materials were examined by using scanning electron microscopy (SEM), where representative electron micrographs were obtained using Jeol, JSM-T20 scanning electron microscope.

2.5. Thermal expansion measurements

The coefficients of thermal expansion of the investigated glasses and glass–ceramics were carried out on 1.5–2.0 cm long rods using a *Linseis L76/1250* automatic recording multiplier Dilatometer with a heating rate of 5 °C/min. The coefficients of thermal expansion of the investigated glasses were measured from room temperature up to 500 °C and the glass–ceramics were measured up to 700 °C. The linear thermal expansion coefficient was automatically calculated using the general equation:

$$\alpha = \frac{\Delta L}{L}\frac{1}{\Delta T}$$

Table 1
Theoretical phase constitution and the respective oxide components of the glasses

Glass no.	Theoretical phase constituents (wt.%)			*R* (Ca-Tschermak's/diopside ratios)	Oxide constitutions (mol%)					
	Dio	Ca-Tsch	FA		SiO_2	Al_2O_3	MgO	CaO	P_2O_5	CaF_2
G_1	75	–	25	0	40.76	–	20.1	33.32	4.36	1.46
G_1a	75	–	25	0	40.76	–	20.1	33.32	4.36	1.46
G_2a	70	5	25	7.14	39.94	1.56	19.36	33.32	4.36	1.46
G_3a	65	10	25	15.38	39.32	3.14	18.40	33.32	4.36	1.46
G_4	60	15	25	25	38.67	4.73	17.46	33.32	4.36	1.46
G_4a	60	15	25	25	38.67	4.73	17.46	33.32	4.36	1.46
G_5a	55	20	25	36.36	37.99	6.49	16.38	33.32	4.36	1.46
G_6	50	25	25	50	37.22	8.16	15.48	33.32	4.36	1.46
G_6a	50	25	25	50	37.22	8.16	15.48	33.32	4.36	1.46

Dio, diopside; Ca-Tsch, Ca-Tschermak; FA, fluorapatite. a = additives: 0.5 g B_2O_3, 2 g Na_2O, 1 g TiO_2

where ΔL is the increase in length, ΔT is the temperature interval over which the sample is heated and L is the original length of the specimen.

2.6. Microhardness measurements

The microhardness of the investigated samples was measured by using *Vicker's* microhardness indenter (*Shimadzu, Type-M, Japan*). The eyepiece on the microscope of the apparatus allowed measurements with an estimated accuracy of $\pm 0.5\,\mu m$ for the indentation diagonals. The specimens were cut using a low speed diamond saw, dry ground using 1200 grit SiC paper and polished carefully using 6, 3 and 1 μm diamond paste to obtain smooth and flat parallel surfaces glass and glass–ceramic samples before indentation testing. At least six indentation readings were made and measured for each sample. Testing was made using a load of 100 g; loading time was fixed for all glasses and crystalline samples (15 s). The measurements were carried out under normal atmospheric conditions. The *Vicker's* microhardness value was calculated from the following equation:

$$H_v = A\left(\frac{p}{d^2}\right)\ \text{kg/mm}^2$$

where A is a constant equal to 1854.5 takes into account the geometry of squared based diamond indenter with an angle 136° between the opposing faces, p is the applied load (g) and d is the average diagonal length (μm). The microhardness values are converted from kg/mm^2 to MPa by multiplying with a constant value 9.8.

3. Results

3.1. Differential thermal analysis

The DTA curves of the studied glasses are presented in Fig. 1. Endothermic reactions at the temperature range of 715–751 °C were recorded on the DTA of the glasses. These endothermic effects are to be attributed to the glass transition (T_g), at which the sample changes from solid to liquid-like behaviour. Various exothermic effects at 912–980 °C indicating crystallization reaction in the glasses are also recorded.

3.2. Crystallization characteristics

The XRD analysis of the crystallization products of the base glass revealed that pyroxene phase of the diopsidic type $CaMgSi_2O_6$ (major lines 3.23, 2.99, 2.95, 2.89, 2.57, 2.52, 2.40, card no.19-239) and fluorapatite phase $Ca_5(PO_4)_3F$, were developed by heating the glass at 720 °C/5h and then at 925 °C/10 h (Fig. 2, pattern I, Table 2).

The addition of minor additives (e.g. $B_2O_3 + Na_2O + TiO_2$) greatly facilitated the melting process and enhanced also the rates of nucleation and crystallization of the glass.

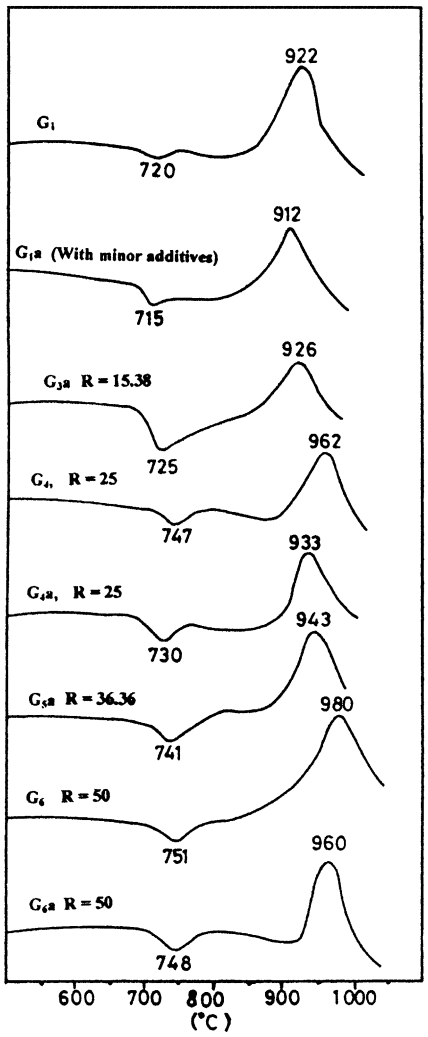

Fig. 1. DTA curves of the studied glasses.

The diopside and fluorapatite phases were greatly enhanced by the addition of minor amount of $B_2O_3 + Na_2O + TiO_2$ as indicated from XRD analysis (Figs. 2 and 3). The progress of crystallization in the glasses, the type and proportion of the resulting crystalline phase assemblages were markedly dependent on the variation of the glass oxide constituents especially the extent of Ca-Tschermak's/diopside replacement.

The DTA (Fig. 1) revealed that the addition of Ca-Tschermak's instead of diopside led to shift both of the endothermic dips and the onset of crystallization exotherms to higher temperatures (e.g. G_3a–G_6a). The DTA traces (Fig. 1) clearly showed also that the addition of minor additives of $B_2O_3 + Na_2O + TiO_2$ to the glasses led to shift both of endothermic and exothermic peak temperatures given by glasses G_4a and G_6a to lower temperatures as compared with those free of additives, i.e. G_4 and G_6.

SEM micrograph (Fig. 4) of the fractured surface of the base glass G_1a (free of Ca-Tschermak's component) showed that fibrous-like growths with some resid-

Table 2
The crystalline phases developed from the crystallized glasses of various Ca-Tschermak's/diopside ratios

Glass no.	Heat treatment	*R* (Ca-Tschermak's/diopside ratios)	Phases developed arranged according to their abundance
G_1	720 °C/5 h to 925 °C/10 h	–	Pyroxene (diopside) + fluorapatite
G_1a	715 °C/5 h to 915 °C/10 h	–	Pyroxene (diopside) increased) + fluorapatite (increased)
G_2a	720 °C/5 h to 920 °C/10 h	7.14	Pyrox. ss. 1 + fluorapatite
G_3a	725 °C/5 h to 925 °C/10 h	15.38	Pyrox. ss. 2 + fluorapatite
G_4	750 °C/5 h to 965 °C/10 h	25.00	Pyrox. ss. 3 + fluorapatite
G_4a	730 °C/5 h to 935 °C/10 h	25.00	Pyrox. ss. 3 + fluorapatite
G_5a	740 °C/5 h to 945 °C/10 h	36.36	Pyrox. ss. 4 + fluorapatite + gehlenite (minor)
G_6	750 °C/5 h to 980 °C/10 h	36.36	Pyrox. ss. 5 + fluorapatite + gehlenite (little)
G_6a	750 °C/5 h to 960 °C/10 h	50.00	Pyrox. ss. 5 + fluorapatite + gehlenite (little)

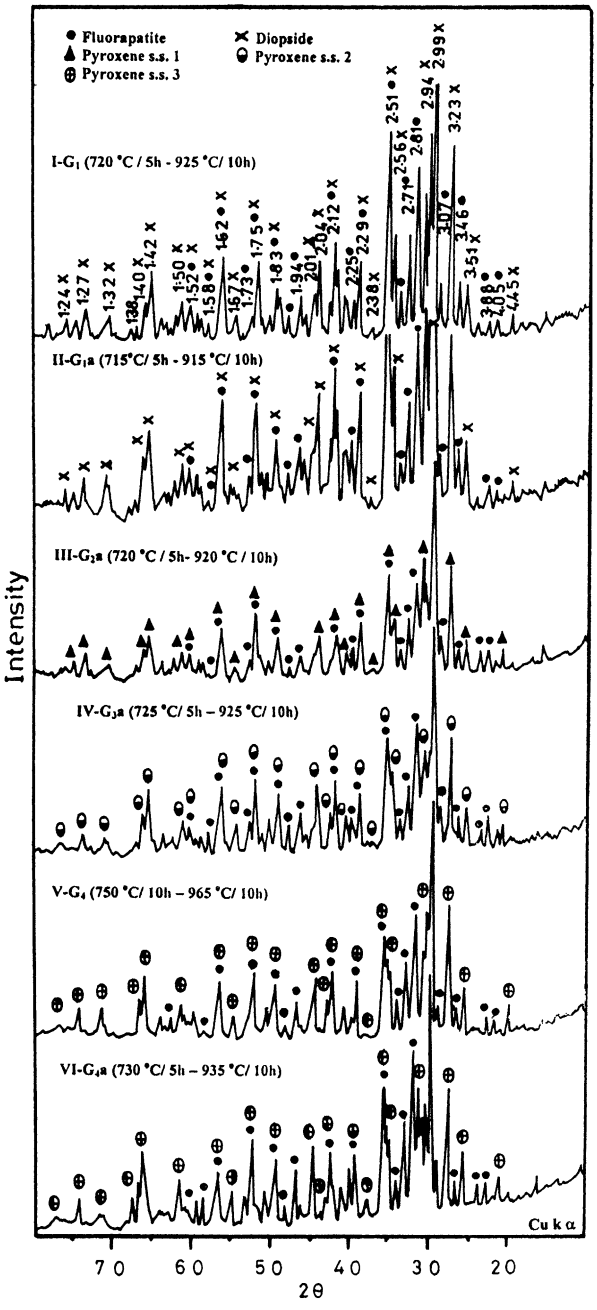

Fig. 2. X-ray diffraction patterns of glasses (G_1–G_4) crystallized at different conditions.

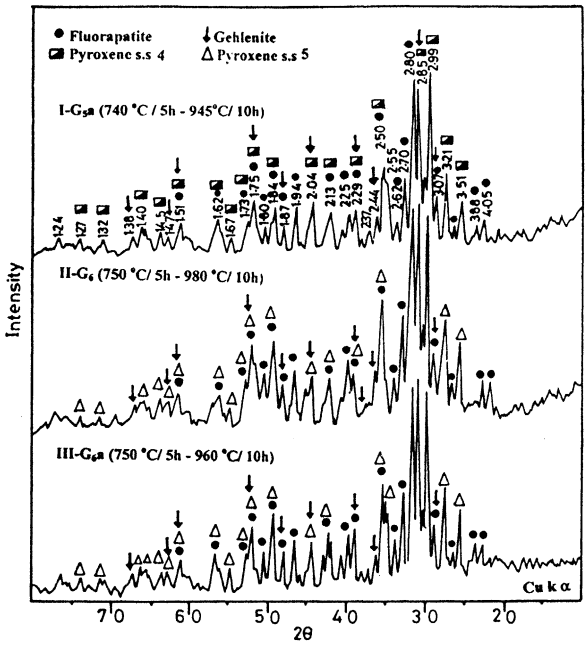

Fig. 3. X-ray diffraction patterns of glasses (G_5–G_6) crystallized at different conditions.

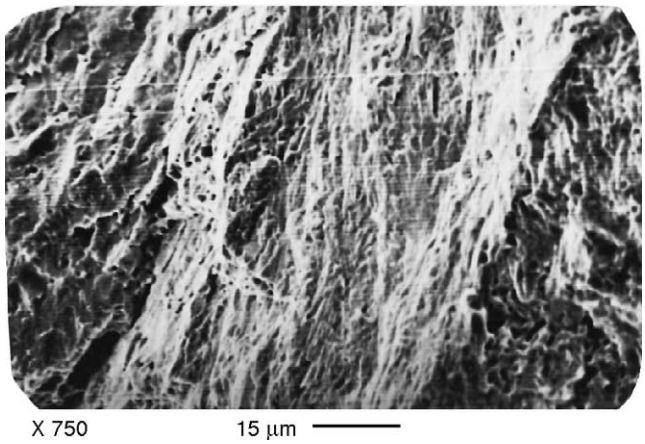

Fig. 4. SEM micrograph of fractured surface of glass G_1a crystallized at 715 °C/5 h to 915 °C/10 h, showing fine fibrous crystals of pyroxene (diopside) and fluorapatite phases with few glassy phase in between.

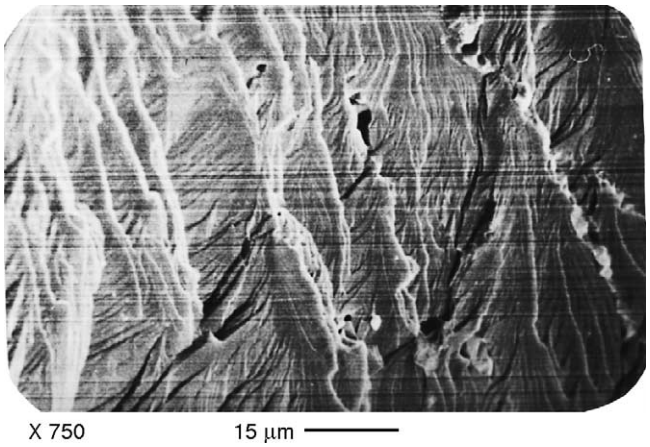

Fig. 5. SEM micrograph of fractured surface of glass G_5a crystallized at 740 °C/5 h to 945 °C/10 h, showing volume crystallization of fine grain microstructure of pyroxene solid solution fluorapatite and gehlenite phases.

ual glassy matrix were developed by crystallization at 715 °C/5 h and then 915 °C for 10 h. However, increasing the Ca-Tschermak's/diopside ratio up to 50, the SEM micrograph (Fig. 5) showed the formation of volume crystallization of fine-grained microstructure in G_5a.

3.3. The effect of Ca-Tschermak's/diopside replacements on the crystalline phases developed

Detailed study for the effect of Ca-Tschermak's/diopside replacement on the crystal phase constitution developed in the glass–ceramic materials (G_2a–G_6a) was performed by the XRD analysis, (Figs. 2 and 3, Table 2). Thermal treatment of the glasses G_2a, G_3a, G_4 and G_4a according to the DTA data led to the formation of pyroxene solid solution of diopsidic type (lines 3.22, 2.98, 2.94, 2.89, 2.55, 2.53, 2.50, 2.04 Å) together with fluorapatite $Ca_5(PO_4)_3F$ (major lines 3.05, 2.80, 2.71 Å, card no.15-876) as proved by the XRD analysis, (Fig. 2, patterns I–VI). While at Ca-Tschermak's/diopside ratio higher than 25%, i.e. G_5a–G_6a, a minor amount of gehlenite phase-$Ca_2Al_2SiO_7$ (major lines 3.47, 3.06, 2.84, 2.41 Å, card no. 35-775) was developed as well (Fig. 3, patterns I–III).

4. Properties

4.1. Thermal expansion

The measurements of the thermal properties, i.e. dilatometric transformation (T_g) and softening (T_s) temperatures as well as the coefficients of thermal expansion (α-values) of the studied glasses and their corresponding glass–ceramic materials were carried out.

The data obtained clearly indicated that the partial addition of Ca-Tschermak's at the expense of diopside in the glass, decreased the α-values of the glasses, and increased

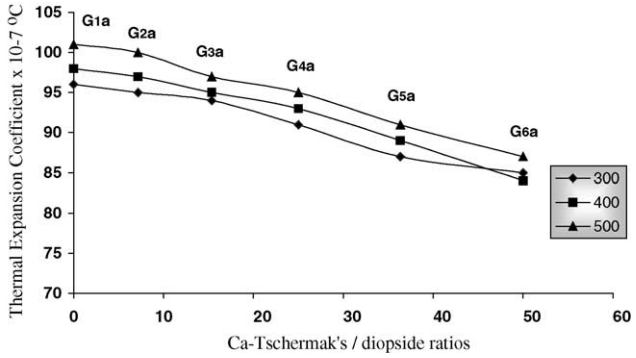

Fig. 6. Thermal expansion coefficient of glass samples with various Ca-Tschermak's/diopside replacement ratios.

their transformation (T_g) and softening (T_s) temperatures. Table 3 and Fig. 6 showed that the expansion coefficients (α) of the glasses were decreased by addition of Ca-Tschermak's at the expense of diopside component. Generally, the addition of $B_2O_3 + Na_2O + TiO_2$ as minor additives increased the expansion coefficient values of the studied glasses and also decreased both the T_g and T_s values as compared with those free of them (Table 3).

The partial replacement of diopside components by Ca-Tschermak's in the glasses (i.e G_1a–G_6a), increased the thermal expansion coefficients of the corresponding crystalline materials, as indicated from Fig. 7, Table 3. Also, the presence of minor additives (i.e. $B_2O_3 + Na_2O + TiO_2$) in the glasses generally increased the α-values of the corresponding glass–ceramics, Table 3.

4.2. Microhardness

Vicker's microhardness property was determined for the glasses and the resulting glass–ceramics. The obtained data revealed that the addition of Ca-Tschermak's at the expense of diopside with different ratios led to an increase in the microhardness values of the glasses (i.e. G_1–G_6, Fig. 8). Also, the addition of $B_2O_3 + Na_2O + TiO_2$ as minor additives in the studied glasses led to decrease the hardness values of the glasses (Table 3).

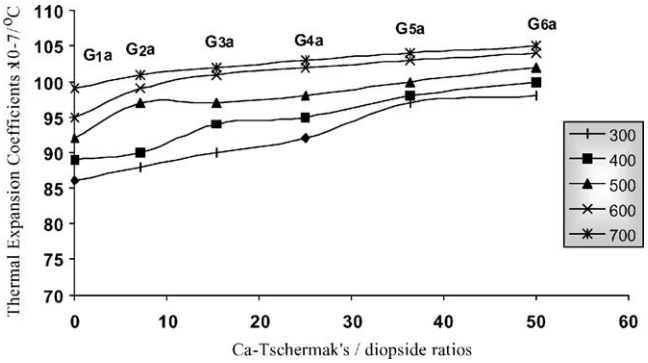

Fig. 7. Thermal expansion coefficient of glass–ceramic samples with various Ca-Tschermak's/diopside replacement ratios.

Table 3
The thermal expansion and microhardness values of various investigated glasses and their corresponding crystalline products

Glass no.	R[a]	Expansion coefficient $\times 10^{-7}$ (/°C)					T_g (°C)	T_s (°C)	Microhardness (Mpa)	Phases developed
		25–300	25–400	25–500	25–600	25–700				
		95	97	98	–	–	677	701	6439	Amorphous
G_1	–	74	76	79	82	90	–	–	6925	Dio + FA
		96	98	101	–	–	652	674	6370	Amorphous
G_1a	–	86	89	92	95	99	–	–	7085	Dio + FA
		95	97	100	–	–	653	681	6676	Amorphous
G_2a	7.14	88	90	97	99	101	–	–	7354	Pyrox. ss.1 + FA
		94	95	97	–	–	659	688	6801	Amorphous
G_3a	15.38	90	94	97	101	102	–	–	7526	Pyrox. ss.2 + FA
		88	90	93	–	–	685	717	7189	Amorphous
G_4	25	86	89	91	94	96	–	–	7693	Pyrox. ss.3 + FA
		91	93	95	–	–	663	692	7037	Amorphous
G_4a	25	92	95	98	102	103	–	–	7814	Pyrox. ss.3 + FA
		87	89	91	–	–	669	702	7212	Amorphous
G_5a	36.36	97	98	100	103	104	–	–	7948	Pyrox. ss.4 + FA + Geh
		82	83	84	–	–	692	713	7487	Amorphous
G_6	50	87	91	94	98	100	–	–	8006	Pyrox. ss.5 + FA + Geh
G_6a	50	85	86	87	–	–	685	709	7383	Amorphous
		98	100	102	104	105	–	–	8055	Pyrox. ss.5 + FA + Geh

Dio, diopside; Pyrox. ss., pyroxene solid solution; Geh, gehlenite; FA, fluorapatite.
[a] R: Ca-Tschermak's/diopside ratios.

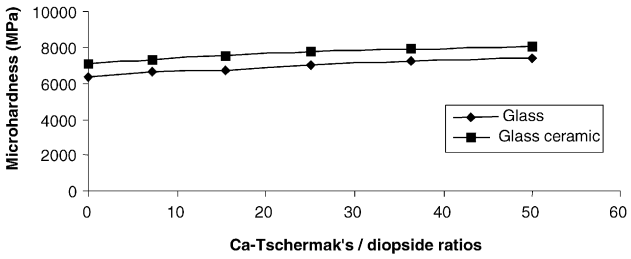

Fig. 8. Microhardness values of the investigated glasses and glass–ceramics with various Ca-Tschermak's/diopside replacement ratios.

For the corresponding crystalline materials, the replacement of diopside by Ca-Tschermak's generally increased the microhardness values of the crystalline samples, i.e. G_2a–G_6a with Ca-Tschermak's as compared with that free of Ca-Tschermak's, i.e. G_1 (Fig. 8, Table 3). The value of sample G_6a with high Ca-Tschermak's/diopside ratio represents the highest value.

5. Discussion

5.1. Crystallization characteristics

The crystallization is the process by which the regular lattice of the crystals is generated from the less well-ordered liquid structure, it is essentially an ordering phenomena.[9] According to the classic theory, crystallization of glass can be viewed as consisting of two distinct stages: nucleation and crystal growth. The first stage (nucleation) takes place near the glass transformation temperature (T_g) and the second stage (crystal growth) occurs above the glass softening point (T_s). The two stages corresponding to different physico-chemical states of glass.[10] It is well known that T_g is influenced by the experimental conditions such as grain size of the sample, heating rate and quenching rate when the sample was prepared.[11]

The addition of $CaAl_2SiO_6$ in the present glasses at the expense of $CaMgSi_2O_6$ had a significant effect on the temperatures at which the nucleation and crystallization start. It increases the temperature of both endothermic and exothermic peaks. The addition of Al_2O_3 causes an increase in the viscosity of the resultant glass melts, which was increased by further addition of Ca-Tschermak's at the expense of diopside in the glass composition.

The ability of aluminium as an intermediate oxide to form the AlO_4 group or to be housed in octahedral coordination as AlO_6 group in the glass interstices is known.[12] The present results indicated that Al^{3+} preferably exhibits a tetrahedral coordination in the studied glasses. The formation of these tetrahedral AlO_4 led to an increase in the viscosity of the glass which hinder the diffusion of different ions and ionic complexes, consequently, it decreases the rate of crystal growth, therefore, some sort of sluggish crystallization of high Al_2O_3 containing glass is expected. Loss of fluorine is likely to be more pronounced in the high fluorine containing glasses. Some of the fluorine present in the starting glass batch can be lost as SiF_4 during melting.[13] However, the formation of (SiF_4) group can be prevented by incorporating Al_2O_3 in the glass melt in which Al^{3+}ion will bond the F^- anion, and this led to hindering the formation of SiF_4 group in the glass.

The addition of $B_2O_3 + Na_2O + TiO_2$ as minor additives in the glass batches facilitated the melting process, relieved the rigidity of the glass structure, lowered the temperature at which the crystallization starts and increasing the crystallization tendency of the glasses. Also, it favoured the development of fine-grained microstructure,[9] as indicated from DTA, XRD and SEM measurements.

McMillan[9] indicated that the addition of TiO_2 as nucleating agent led to the formation of fine-grained microstructure specially when it was added to Al_2O_3 or CaO containing silicate glasses. On the other hand, $B_2O_3 + Na_2O$ were used as fluxing agents to facilitate the melting process and increasing the homogeneity of the glasses.[14]

Pyroxene consists of a group of minerals of variable compositions, which crystallize fairly readily. They are closely related in crystallographic and other physical properties, as well as in chemical composition.[15]

The pyroxenes have a wide range of chemical composition. The complexity of this group is exhibited by the wide isomorphism of the various elements in the expandable pyroxene formula:

$$W_{1-p}(X, Y)_{1+p}Z_2O_6$$

where *W*: Ca, Na; *X*: Mg, Fe^{2+}, Mn, Zn, Li; *Y*: Al^{3+}, Fe^{3+}, Cr, Ti; *Z*: Si, Al, Fe^{3+} and *p*: number of ions.

A wide variety of ionic substitutions occur in the members of the pyroxene group and there is a complete replacement between some of the group components. The limits of the isomorphous substitution by the different ions in the pyroxene structures depend mainly on two factors:

1. The compositions of the initial host pyroxene crystal, i.e. the nature of those elements sharing in the building of the initial host pyroxene crystal.
2. The conditions of crystallization, namely the degree of equilibria of the mineral-forming process.

The occurrence of the various phases formed in the present glasses was function of the Ca-Tschermak's/diopside ratios in the glasses and the crystallization parameters used. At low Ca-Tschermak's content, i.e. G_2a with Ca-Tschermak's/diopside ratio equals 7.14, pyroxene solid solution of diopsidic type was formed together with fluorapatite phase. It seemed that, the diopside phase $CaMgSi_2O_6$ goes into solid solution with the Ca-Tschermak's $CaAl_2SiO_6$ to form pyroxene solid solution ($CaMgSi_2O_6$–$CaAl_2SiO_6$), i.e. there is a preferential tendency for diopside to capture Ca-Tschermak's in its structure forming pyroxene solid solution of diopsidic type.

Kushiro[16] determined the maximum concentrations of the $CaAl_2SiO_6$ component, which can be taken up by diopside as 20%. Omar et al.,[17] showed that complex pyroxene containing up to 48% of the $CaAl_2SiO_6$ component under non-equilibrium conditions of crystallization could be obtained. Ca-Tschermak ($CaAl_2SiO_6$) is a pyroxene phase. The amount of aluminium sharing in the pyroxene structure is dependent upon the original composition of the glass and the crystallization parameters. Flemming and Luth[18] studied the system $CaMgSi_2O_6$–$CaAl_2SiO_6$. They showed that the composition across the diopside–Ca-Tschermak's solid solution follow the general formula:

$$\underset{\text{Octahedral sublattice}}{Ca[Mg_{1-x}, Al_x]}\underset{\text{Tetrahedral sublattice}}{(Si_{(1-x)/2}, Al_{x/2})_2O_6}$$

The displacement of the major characteristics *d*-spacing lines of the pyroxene variety towards higher 2θ values may support the suggestion that the Al^{3+} was incorporated in the pyroxene ss of diopsidic type. Theoretically,[19] it is assumed therefore, that the aluminous pyroxenes ss phase (Pyrox. 1) formed in the glass–ceramic of G_2a has probably the following formula:

$$Ca(Mg_{0.94}, Al_{0.06})(Si_{0.96}, Al_{0.04})_2O_6$$

For sample G_3a the replacement of diopside by Ca-Tschermak's up to ratio 15.38, giving rise to the development of the aluminous pyroxene ss phase (Pyrox. 2) which has the probable formula:

$$Ca(Mg_{0.87}, Al_{0.13})(Si_{0.93}, Al_{0.07})_2O_6$$

On increasing the Ca-Tschermak's/diopside replacements up to ratio 25 (i.e. sample G_4), the resulting aluminous pyroxene ss phase (Pyrox. 3) may exhibit the following formula:

$$Ca(Mg_{0.8}, Al_{0.2})(Si_{0.90}, Al_{0.1})_2O_6$$

The recalculation of the glass compositions of G_2–G_4 to normative mineral molecules revealed that the limit of the isomorphous substitution of Ca-Tschermak's component $CaAl_2SiO_6$, accommodated in diopside $CaMgSi_2O_6$ structure to form aluminous pyroxene ss was 25%.

There was no evidence for the formation of solid solution between diopside or Ca-Tschermak's and fluorapatite crystals and this was in agreement with the results obtained by Tulyaganov.[4]

The XRD patterns revealed also that on increasing Ca-Tschermak's at the expense of diopside up to ratio 36.36 and 50, i.e. glasses G_5a and G_6a, respectively, gehlenite $Ca_2Al_2SiO_7$ phase was developed as well. The theoretical calculation of these glass compositions into normative mineral molecules[19] indicated that the complex pyroxenes formed in samples G_5 and G_6, contain more than 25% of $CaAl_2SiO_6$ component in its structure.

The present result revealed that an increase of Ca-Tschermak's component above 25%, which corresponds to 6.49 and 8.16 mol% of Al_2O_3 in diopside structure in samples G_5 and G_6 led to the crystallization of gehlenite–$Ca_2Al_2SiO_7$ phase together with the aluminous pyroxene ss phases. The probable formulae of pyroxene ss phases in samples G_5 and G_6 are difficult to be calculated due to the formation of gehlenite phase ($Ca_2Al_2SiO_7$) among the crystallization products of these glasses.

Gehlenite phase is related to a group of minerals known as melilite. The chemical formula of the melilite group is a solid solution of Al-end member gehlenite $Ca_2Al_2SiO_7$ and Mg-end member akermanite $CaMgSi_2O_7$.[20]

Schairer and Yoder,[21] studied the system $CaMgSi_2O_6$–$CaAl_2SiO_6$. They showed that the maximum solubility of the Ca-Tschermak's pyroxene molecule $CaAl_2SiO_6$ in diopside $CaMgSi_2O_6$ is 20%, and that anorthite and melilite solid solutions are always present in the crystalline phases of the compositions greater than 20 wt.% of $CaAl_2SiO_6$.

5.2. Thermal expansion

The thermal expansion of glass is not only a function of temperature, but also depends on other factors such as composition, structure of the glass, e.g. degree of polymerization, type of structural units, the nature and contribution of the different cations, whether they occupy forming or modifying positions in the glass network. Accordingly, the thermal expansion data can yield valuable information regarding, for example the structural changes induced by modification of composition or heat treatment.[22] Materials of high hardness, right expansion behaviour and good biocompatibility are used as artificial implants in orthopedic surgery.[5] To realize that the addition of $CaAl_2SiO_6$ instead of $CaMgSi_2O_6$ decreases the thermal expansion coefficients and increases the T_g and T_s values of the present glasses, the role of Al^{3+} coordination in the glass structure must be considered, which seems to change its coordination from AlO_6 octahedral to AlO_4 tetrahedral. This is associated with a change in bonding character with a simultaneous increase in the tightness of the structure, resulted into a decrease in the expansion coefficient and increase in both the T_g and T_s values of the investigated glass.[22]

The addition of $B_2O_3 + Na_2O + TiO_2$ as minor additives in glass compositions increased the α-values and lowered both T_g and T_s of the studied glasses. This may be explained on the basis that these additives relieved the rigidity of the glass structure, which led to increase the lattice vibration and caused an increase in the relative contribution of the anharmonicity term,[23] i.e. an increase in the α-values and a decrease in both T_g and T_s values could be expected.

The thermal expansion of crystalline solids can be markedly different from those of the parent glasses. The crystallization process greatly altered the thermal expansion of the glasses. Therefore, the glass–ceramic materials may have high or low coefficients of expansion depending on the expansion coefficient and elastic properties of the crystal phases formed, including the residual glass matrix.[24] In most cases, the expansion coefficients of the crystalline materials generally increase with increasing glassy phase contents in the materials.

An extremely wide range of thermal expansion coefficients (α) is covered by the different crystal types and the development of these phases in appropriate proportions forms the basis of the production of glass–ceramics with controlled thermal expansion coefficients. It has been reported that pyroxenes had high positive values of their expansion coefficients. Diopside and Ca-Tschermak's which are considered to be pyroxene members have α-values of (50–150) $\times$ $10^{-7}\,^{\circ}C^{-1}$ (20–800 °C)[9] and 88 $\times$ $10^{-7}\,^{\circ}C^{-1}$ (20–1200 °C), respectively.[25] Melilite group, e.g. gehlenite has α-values of 123 $\times$ $10^{-7}\,^{\circ}C^{-1}$ (20–1000 °C).[26] While fluorapatite has α-values of (74–119) $\times$ $10^{-7}\,^{\circ}C^{-1}$ (20–300 °C).[27] Abe[28] revealed that the natural tooth enamel has thermal expansion coefficient of 114 $\times$ $10^{-7}\,^{\circ}C^{-1}$ (20–400 °C).

Accordingly, the α-values of the crystalline samples (G_1–G_6) increased with increasing Ca-Tschermak's/diopside replacement ratios. This may be due to the formation of relatively higher thermally expanding aluminous pyroxene solid solutions instead of the diopside phase. This means that aluminous pyroxene ss has α-value higher than that of diopside phase. A contribution of a particular crystal phase to the thermal expansion of a glass ceramic may be modified if the crystal phase enters into solid solution with another phase.[9]

The development of relatively high expanding gehlenite phase together with aluminous pyroxene ss and fluorapatite phases in samples of G_5a–G_6a, led to a further increase in the α-values of the gehlenite containing samples (G_5a–G_6a) as compared with those free of it (G_2a–G_4a).

The higher α-values of the samples containing $B_2O_3 + Na_2O + TiO_2$ than those free of these additives can be explained by assuming that maximum amounts of B_2O_3 and Na_2O were present in the glassy matrix which contains enough non-bridging ions,[14] giving rise to a less coherent network and subsequently a higher expansion coefficient value.

5.3. Hardness

The microhardness of the material is often equated with its resistance to abrasion or wear and this characteristic is of practical interest since it may determine the durability of a material during use and it may also decide the suitability of the material for special applications.[24]

In the hardness indentation process, the glass is assumed to undergo both compression and shear[29] These two processes produce stresses, which are primarily responsible for the various deformations, which in turn give rise to the formation of observed indentations. Among the deformations, which are believed to be caused by one or the combination of the two stresses, the following have been experimentally observed in glasses: (a) viscous or plastic flow due to shear; (b) elastic deformation caused by compression; and (c) densification resulting from compression and shear which in some cases may involve breaking of bonds.

Varshneya[30] revealed that the addition of alkalies to the silicate glasses decreased their hardness presumably because the connectivity of the glass structure decreased. Scholze[31]

revealed that, using viscosity as an analogy, the addition of alkalies would decrease the hardness of the glasses.

The addition of $CaAl_2SiO_6$ component at the expense of $CaMgSi_2O_6$ markedly increases the hardness values of the glasses (G_1–G_6). MacDowell[12] revealed that because of the strong network forming role of Al_2O_3 in aluminosilicate glasses, their viscosities over a wide range of temperatures increase as the $Al_2O_3/(M_2O + MO)$ ratio increases up to a value of unity. Since there is a direct relationship between hardness and viscosity, high Al_2O_3 containing glasses display high hardness values. According to Miska[32] the microhardness of crystallized glasses depends not only on the type of precipitating phases but also on their size, shape, natural wetting and on the emergence or absence of internal cracks. However, the degree of crystallinity should be also taken into consideration.

The microstructure represents the major role in determining the microhardness values of the crystalline glasses.[33] Sohn et al.,[34] revealed that the hardness of silicate glass–ceramics increased due to the fine-grained microstructure by which the crystal size play an important role in preventing the propagation of the cracks in the whole structure.

The present results revealed that the addition of Ca-Tschermak's component instead of diopside led to increase the hardness values of the investigated glass–ceramics (G_1–G_6). This can be attributed to the formation of fine-grained microstructure in the investigated glass–ceramics. SEM micrograph clearly showed that the glass–ceramic of sample G_5a (with 20% Ca-Tschermak's) exhibits a very fine-grained microstructure (Fig. 5) as compared with the base glass G_1a (free of Ca-Tschermak's contents, Fig. 4).

6. Conclusions

Varieties of pyroxene solid solutions series together with fluorapatite and gehlenite phases could be formed in glass–ceramics based on diopside–Ca-Tschermak's–fluorapatite glass compositions. The limit of the isomorphous substitution of Ca-Tschermak's component, $CaAl_2SiO_6$, that accommodated in diopside $CaMgSi_2O_6$ structure to form aluminous pyroxene solid solution was 25%. Above this limit gehlenite ($Ca_2Al_2SiO_7$) phase was formed as well.

The addition of $CaAl_2SiO_6$ at the expense of $CaMgSi_2O_6$ decreases the α-values and increases the T_g, T_s and microhardness values of the present glasses, while the α-values and the microhardness of the crystalline samples increased with increasing Ca-Tschermak's/diopside ratios. The data of the glasses were correlated to the internal structure of the glasses, nature and role played by glass-forming cations, however, for the glass–ceramics, the crystalline phases formed the residual glassy matrix and microstructure are considered.

References

1. Rogers, P. S., The initiation of crystal growth in glasses. *Mineral. Magn.* 1970, **37**(291), 741–758.
2. Berezhnoi, A. I., *Glass–Ceramics and Photositalls*. Plenum Press, NY, 1970.
3. Erol, M., Kucukbayrak, S., Ersoy-Mericboyu, A. and Avecoglu, M. L., Crystallization behaviour of glasses produced from fly ash. *J. Eur. Ceram. Soc.* 2001, **21**(16), 2835–2841.
4. Tulyaganov, D. U., Phase separation and devitrification in the fluorapatite–diopside system. In *XIX Proceeding of the International Congress on Glass, Vol 2, Extended Abstract*. Edinburgh, Scotland, 1–6 July 2001, p. 198.
5. Tulyaganov D. U., Aripova, M., Bioactive glass–ceramic containing anorthite and diopside. *XVI Proc. Inter. Congr. Glass, Bol. Soc. ESP Ceram. VID 31-C*, 1992, **5**, 227–232.
6. Stanton, K. and Hill, R., The role of fluorine in the devitrification of SiO_2–Al_2O_3–P_2O_5–CaO–CaF_2 glasses. *J. Mater. Sci.* 2000, **35**, 1911–1916.
7. Szabo, I., Nagy, B., Volksch, G. and Holland, W., Structure chemical durability and hardness of glass–ceramics containing apatite and leucite crystals. *J. Non-Cryst. Solids* 2000, **272**, 191.
8. Holland, W., Rheinberger, V. and Frank, M., Mechanisms of nucleation and controlled crystallization of needle-like apatite in glass–ceramics of the SiO_2–Al_2O_3–K_2O–CaO–P_2O_5 system. *J. Non-Cryst. Solids* 1999, **253**, 170.
9. McMillan P. W. *Glass–Ceramics*. Academic Press, London, 1979.
10. Stoch, L., Structure and crystallization of multicomponent glasses. In *XIX Proc. Inter. Congr. Glass, Vol 1, Invited Papers*. Edinburgh, Scotland, 1–6 July 2001, pp. 62–73.
11. Nishida, T., Hirai, T. and Takashima, Y., Mossbauer and DTA studies of the crystallization of borosilicate glasses. *Phys. Chem. Glasses* 1983, **24**(5), 113–116.
12. MacDowell, J. F., Alumina in glasses and glass–ceramics, reprinted from alumina chemicals science and technology handbook. *Am. Ceram. Soc., Inc.*, 1990, 365–374.
13. Hill, R. G., Goat, C. and Wood, D., Thermal analysis of SiO_2–Al_2O_3–CaO–CaF_2 glass. *J. Am. Ceram. Soc.* 1992, **75**, 778–782.
14. Zarzycki, J., *Glass and Vitreous State*. Cambridge University Press, NY, 1991.
15. Deer, W. A., Howie R. A. and Zussman J., *An Introduction to the Rock Forming Minerals* (*2nd ELBS ed.*). Hong Kong Printing Press Ltd., 1992.
16. Kushiro, Y., Clinopyroxenes solid solutions. Part 1. The $CaAl_2SiO_6$ component. *Jpn. J. Geol. Geography* 1962, **33**, 2–4.
17. Omar, A. A., Salman, S. M. and Mahmoud, M. Y., Phase relations in the diopside anorthite–akermanite system. *Ceram. Int.* 1986, **12**, 53–59.
18. Flemming, L. R. and Luth, R. W., ^{29}Si MAS NMR study of diopside–Ca-Tschermak clino-pyroxenes: detecting both tetrahedral and octahedral Al substitution. *Am. Mineral.* 2002, **87**, 25–36.
19. Barth T. F., *Theoretical Petrology* (*2nd ed.*). Wiley, NY, 1962.
20. Morioka, M., Kamata, Y. and Nagasawa, H., Diffusion in single crystals of melilite III. Divalent cations in gehlenite. *Geochim. Cosmochim. Acta* 1997, **61**, 1009–1016.
21. Schairer, J. F. and Yoder, Jr. H.S., Crystal and liquid trends in simplified alkali basalts. *Year Book* 1964, **63**, 64–74.
22. Salama, S. N. and Salman, S. M., Contribution of manganese oxide to the thermal expansion of some silicate glasses and their crystalline solids. *Thermochim. Acta* 1991, **191**, 187–199.
23. Feltz, A., *Amorphous Inorganic Materials and Glasses*. VCH Publishers, Inc., NY, 1993.
24. Holland, W., Beall, G. H., Glass–ceramic technology. *Am. Ceram. Soc. Inc.*, 2002.
25. Haselton, J., Hemingway, B. S. and Robie, R. A., Low-temperature heat capacities of $CaAl_2SiO_6$ glass and pyroxene and thermal ex-

pansion of $CaAl_2SiO_6$ pyroxene. *Am. Mineral.* 1984, **69**, 481–489.
26. Hemingway, B. S. and Robie, R. A., Heat capacity and thermodynamic function for gehlenite and sturolite with comments on the Schottky anomaly in the heat capacity of sturolite. *Am. Mineral.* 1984, **69**, 307–318.
27. Vogel, W., Holland, W., Naumann, K. and Gummel, J., Development of machineable bioactive glass–ceramics for medical uses. *J. Non-Cryst. Solids* 1986, **80**(1–3), 34–51.
28. Abe, Y., Glass ceramics based on calcium phosphates, artificial dental crown and micro-porous glass–ceramics. *Glastech-Ber. Glass. Sci. Technol.* 2000, **73C1**, 286–292.
29. Yamane, M. and Mackenzie, J. D., Vicker's hardness of glass. *J. Non-Cryst. Solids* 1974, **15**(2), 153–164.
30. Varshneya, A. K., *Fundamentals of Inorganic Glasses*. Academic Press, London, 1994.
31. Scholze, H., *Glass: Nature, Structure and Properties*. Springer-Verlage, NY, 1990.
32. Miska, H. A. Ceramics and glasses. In *Engineering Material Handbook, Vol 4*. ASM International, 1991.
33. Park, Y. J., Moon, S. O. and Heo, J., Crystalline phase control of glass–ceramics obtained from sewage sludge fly ash. *Ceram. Int.* 2003, **29**(2), 223–227.
34. Sohn, S. B., Choi, S. Y. and Lee, Y. K., Controlled crystallization and characterization of cordierite glass–ceramics for magnetic memory disk substrate. *J. Mater. Sci* 2000, **35**, 4815–4821.